Contribution from the Department of Chemistry,
University of Massachusetts, Amherst, Massachusetts 01003

Hydrogen-Bonded Chain and Dimer Formations of Spirocyclic Tetraoxyphosphoranes Possessing Phosphorinane Chair Conformations[1]

Johannes Hans, Roberta O. Day, and Robert R. Holmes*

Received February 21, 1991

Oxidative-addition reactions of aminophenols with the monocyclic phosphite $(Me_2C_3H_4O_2)P(O\text{-}Xyl)$, yielded new spirocyclic tetraoxyphosphoranes containing saturated six-membered rings, $(Me_2C_3H_4O_2)(O_2NC_6H_3ONH)P(O\text{-}Xyl)$ (**1**), $(Me_2C_3H_4O_2)(C_5H_3NONH)P(O\text{-}Xyl)$ (**2**), and $(Me_2C_3H_4O_2)(Me_2C_6H_2ONH)P(O\text{-}Xyl)$ (**4**). Hydrogen bonding was introduced via N-H---X (X = O, N) interactions involving remote ring substituents to ascertain their influence as a structural determinant. X-ray analysis revealed phosphoranes in trigonal-bipyramidal geometries with rings situated in axial-equatorial sites. A hydrogen bonded chain structure was obtained for **1** with the phosphorinane ring in a chair conformation. For **2**, a hydrogen-bonded dimer was found with the six-membered ring in a twisted or half-chair form. Reaction of 2-hydroxybenzyl alcohol with $(Me_2C_3H_4O_2)P(O\text{-}Xyl)$ gave the phosphate formation $(Me_2C_3H_4O_2)P(O)(O\text{-}Xyl)$ (**3**), confirmed by X-ray analysis with the ring in a chair conformation. Variable-temperature ^1H NMR spectroscopy showed fluxional molecules undergoing intramolecular ligand exchange via a TBP exchange intermediate with the six-membered ring located in diequatorial sites. Activation energies in the range 10.5-12.5 kcal/mol were obtained. The relevance of the results to pentaoxyphosphorane intermediates proposed in c-AMP enzyme reactions is cited. **1** crystallizes in the monoclinic space group $P2_1/c$ with a = 8.1618 (9) Å, b = 20.240 (4) Å, c = 12.577 (1) Å, β = 103.26 (1)°, and Z = 4. **2** crystallizes in the monoclinic space group $P2_1/n$ with a = 11.200 (2) Å, b = 27.347 (8) Å, c = 12.865 (3) Å, β = 105.23 (2)°, and Z = 8. **3** crystallizes in the orthorhombic space group $P2_12_12_1$ with a = 7.253 (1) Å, b = 9.456 (2) Å, c = 20.510 (3) Å, and Z = 4. The final conventional unweighted residuals are 0.037 (**1**), 0.050 (**2**), and 0.035 (**3**).

Introduction

Previous work has shown that cyclic five-coordinated phosphorus compounds that contain saturated six-membered rings normally have these rings present in boat conformations located in axial-equatorial sites of a trigonal bipyramid (TBP).[1b,2-10] This conformation is the most favorable one in that it allows the endocyclic equatorial heteroatom bonded to phosphorus to orient its lone pair in the equatorial plane.[11] The requirement is that the plane of the P-X_{eq}-C ring atoms be at 90° to the equatorial plane. On the basis of model calculations, Trippett[11] has shown that the boat conformation is the only one that meets this requirement.

Recent work in our laboratory has provided exceptions to this conformational preference when additional features are present in the phosphorane molecules. In one study the introduction of hydrogen-bonding possibilities resulting from the use of aminophenol reactants led to the spirocyclic tetraoxyphosphoranes A-C,[12] which from X-ray analysis had the phosphorinane rings

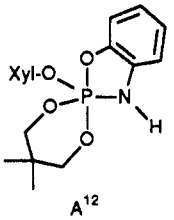

A[12]

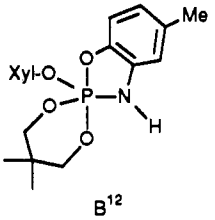

B[12]

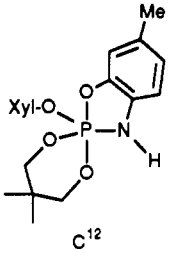

C[12]

appear in chair conformations while their axial-equatorial orientations were maintained in TBP structures. For A, the six-membered ring resided in a chair conformation in a hydrogen-bonded helical chain arrangement whereas both B and C exhibited hydrogen-bonded dimer formations where chair and boat conformations coexisted.

The only additional example of a chair conformation was found for this same ring similarly oriented in the monocyclic tetraoxyphosphorane D,[1b] which contained the pentafluorophenoxy ligands,

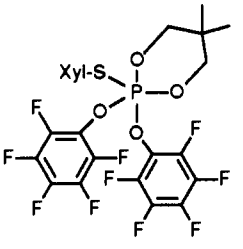

D[1b]

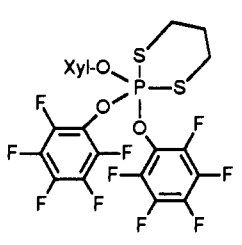

E[1b]

C_6F_5O. The related sulfur-containing ring derivative E[1b] had the thiophosphorinane ring in a boat conformation. A combination of an electronegativity effect and a steric effect associated with the sizeable C_6F_5O ligand was reasoned[1b] to stabilize the chair conformation in D.

For all of the tetra- and pentaoxyphosphoranes containing saturated six-membered rings that have been studied by X-ray analysis, which now number approximately 15, none have been found to have the phosphorinane positioned at diequatorial sites of a TBP. The same is found true for the few derivatives studied that contain six-membered rings with nitrogen[7,10] and sulfur[1b,3] heteroatoms and those that possess larger rings[4,5] with ring oxygen atoms bound to phosphorus. The rings invariably have appeared at axial-equatorial sites of a TBP. Diequatorial ring orientation from an experimental basis has been advanced only in the case of NMR studies of phosphoranes by Broeders et al. (F)[13] and Abdou et al. (G, H).[14]

Pentacoordinated cyclic phosphorus compounds of the type discussed here, A-D and F, serve as models for proposed activated states in cyclic adenosine 3',5'-monophosphate (*c*-AMP) action.

(1) (a) Pentacoordinated Molecules. 89. (b) Part 88: Hans, J.; Day, R. O.; Howe, L.; Holmes, R. R. *Inorg. Chem.* **1991**, *30*, 3132.
(2) Schomburg, D.; Hacklin, H.; Röschenthaler, G.-V. *Phosphorus Sulfur* **1988**, *35*, 241.
(3) Kumara Swamy, K. C.; Holmes, J. M.; Day, R. O.; Holmes, R. R. *J. Am. Chem. Soc.* **1990**, *112*, 6092 and references cited therein.
(4) Kumara Swamy, K. C.; Day, R. O.; Holmes, J. M.; Holmes, R. R. *J. Am. Chem. Soc.* **1990**, *112*, 6095.
(5) Burton, S. D.; Kumara Swamy, K. C.; Holmes, J. M.; Day, R. O.; Holmes, R. R. *J. Am. Chem. Soc.* **1990**, *112*, 6104.
(6) Kumara Swamy, K. C.; Burton, S. D.; Holmes, J. M.; Day, R. O.; Holmes, R. R. *Phosphorus, Sulfur Silicon* **1990**, *53*, 437.
(7) Holmes, R. R.; Kumara Swamy, K. C.; Holmes, J. M.; Day, R. O. *Inorg. Chem.* **1991**, *30*, 1052.
(8) Yu, J. H.; Sopchik, A. E.; Arif, A. M.; Bentrude, W. G. *J. Org. Chem.* **1990**, *55*, 3444.
(9) Yu, J. H.; Arif, A. M.; Bentrude, W. G. *J. Am. Chem. Soc.* **1990**, *112*, 7451.
(10) Barlow, J. H.; Bone, S. A.; Russell, D. R.; Trippett, S.; Whittle, P. J. *J. Chem. Soc., Chem. Commun.* **1976**, 1031.
(11) Trippett, S. *Pure Appl. Chem.* **1974**, *40*, 595.
(12) Day, R. O.; Kumara Swamy, K. C.; Fairchild, L.; Holmes, J. M.; Holmes, R. R. *J. Am. Chem. Soc.* **1991**, *113*, 1627.
(13) Broeders, N. L. H. L.; Koole, L. H.; Buck, H. M. *J. Am. Chem. Soc.* **1990**, *112*, 7475.
(14) Abdou, W. M.; Denney, D. B.; Denney, D. Z.; Pastor, S. D. *Phosphorus Sulfur* **1985**, *22*, 99.

0020-1669/91/1330-3928$02.50/0

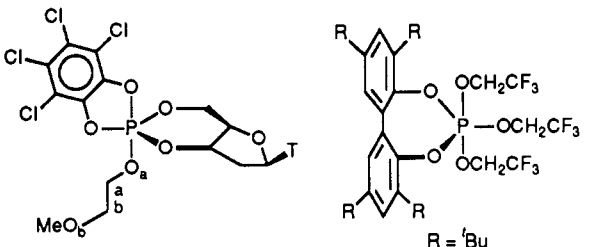

F[13]

R = tBu
R = H
G[14]

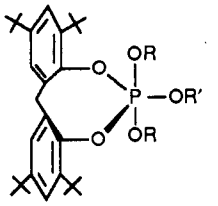

R = R' = CH_2CF_3
R = CH_2CF_3; R' = C_2H_5
H[14]

Specifically, it has been proposed by Buck and co-workers[13,15,16] that a P^V-TBP intermediate with the 3',5'-dioxaphosphorinane ring of *c*-AMP located diequatorially in a TBP is involved in triggering action of protein kinases which leads to a cascade of enzymatic reactions that ultimately causes a breakdown of glycogen and the release of glucose to the blood stream. In the case of the interaction of phosphodiesterases with *c*-AMP, a P^V-TBP intermediate with the phosphorinane ring located in axial–equatorial positions has been proposed.[16] These enzymes catalyze the hydrolysis of *c*-AMP to 5'-AMP. In view of the importance of establishing mechanistic features of these enzymatic processes, it is imperative to define the underlying basis regarding structural preferences of isolatable cyclic oxyphosphoranes containing compositions related to *c*-AMP-proposed activated states.

In the present paper, the role of hydrogen bonding, which represents an important active-site constraint, is expanded as a structural determinant by conducting the synthesis, X-ray analysis, and NMR study of the spirocyclic tetraoxyphosphoranes **1** and **2** and comparison with similar studies of the tetracoordinated cyclic phosphate **3**. In addition, the synthesis and NMR study of the related tetraoxyphosphorane **4** was accomplished.

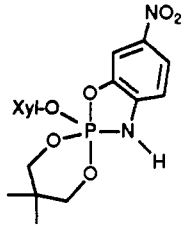

1

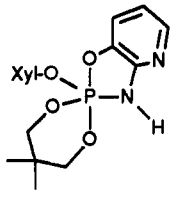

2

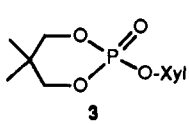

3

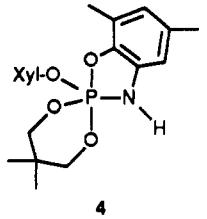

4

Experimental Section

Chemicals used were obtained from Aldrich and Fluka and used without further purification. Solvents used were freshly distilled. Diethyl ether and tetrahydrofuran were dried over sodium/benzophenone until a blue color persisted. Acetone and hexane were refluxed over phosphorus pentoxide. Nitrogen was purified with the use of a copper catalyst and subsequently dried in a phosphorus pentoxide column.

^1H and ^{31}P NMR spectra were recorded on a Varian XL 300 FT-NMR spectrometer. Chemical shifts for ^{31}P NMR spectra were obtained by setting triphenyl phosphate ($CDCl_3$) at −18 ppm[17] and referenced to 85% orthophosphoric acid. All chemical shifts are reported at 18 °C unless otherwise noted. Negative shifts are upfield.

Syntheses. 2-(2,6-Dimethylphenoxy)-5',5'-dimethyl-6-nitrospiro[1,3,2-benzoxazaphosphole-2(3*H*),2'λ⁵-[1,3,2]dioxaphosphorinane], ($Me_2C_3H_4O_2$)($O_2NC_6H_3ONH$)P(O-Xyl) (1). 2-Amino-5-nitrophenol (1.09 g, 7.13 mmol) and 2-(2,6-dimethylphenoxy)-5,5-dimethyl-1,3,2-dioxaphosphorinane, prepared as previously described,[4] were dissolved in diethyl ether (75 mL). *N*-Chlorodiisopropylamine (0.96 g, 7.13 mmol) was added and the solution stirred for 5 h. Diisopropylamine hydrochloride was filtered off, and the solvent was removed under reduced pressure until crystallization occurred. The solution was left in the refrigerator at −6 °C for 1 day. Yellow crystals resulted, mp 179–180 °C (0.98 g, 34%). ^1H NMR (CD_2Cl_2, ppm, 17.5 °C): 0.94 (s, 3 H, OCH_2CH_3), 1.18 (s, 3 H, OCH_2CH_3), 2.15 (s, 6 H, $C_6H_3(CH_3)_2$), 3.87 (dd, $^3J(P-H_x)$ = 35.7 Hz, $^2J(H_A-H_x)$ = 16.2 Hz, 2 H, $OCH_2(X)$), 4.25 (t or dd, $^3J(P-H_A)$ = $^2J(H_A-H_x)$ = 14.5 Hz, 2 H, $OCH_2(A)$), 5.29 (impurity), 6.24 (d, $^2J(P-H)$ = 30.4 Hz, 1 H, N*H*), 6.70–7.70 (m, 6 H, H_{aryl}). ^{31}P NMR ($CDCl_3$, ppm): −59.17. Anal. Calcd for $C_{19}H_{23}O_6N_2P$: C, 56.16; H, 5.70; N, 6.89. Found: C, 56.05; H, 5.76; N, 6.78.

2-(2,6-Dimethylphenoxy)-5',5'-dimethylspiro[1,3,2-pyrido[2,3-*d*]oxazaphosphole-2(3*H*),2'λ⁵-[1,3,2]dioxaphosphorinane], ($Me_2C_3H_4O_2$)(C_5H_3NONH)P(O-Xyl) (2). To a suspension of 2-(2,6-dimethylphenoxy)-5,5-dimethyl-1,3,2-dioxaphosphorinane (1.6 g, 6.3 mmol) and 2-amino-3-hydroxypyridine (0.69 g, 6.3 mmol) in tetrahydrofuran (75 mL) was added *N*-chlorodiisopropylamine (0.85 g, 6.3 mmol). The reaction mixture was stirred at room temperature for 2 h. Sodium hydride (0.16 g, 6.3 mmol) was added in small portions. An exothermic reaction occurred with the formation of hydrogen. After 1 h the precipitate was filtered off and the solution concentrated to 15 mL under reduced pressure. Layering the resulting solution with diethyl ether (10 mL) afforded colorless needles, mp 231–235 °C dec (1.2 g, 52.6%). ^1H NMR (CD_2Cl_2, ppm): 0.98 (s, 3 H, OCH_2CH_3), 1.19 (s, 3 H, OCH_2CH_3), 2.19 (s, 6 H, $C_6H_3(CH_3)_2$), 3.90 (dd, $^3J(P-H_x)$ = 22.9 Hz, $^2J(H_A-H_x)$ = 10.7 Hz, 2 H, $OCH_2(X)$), 4.22 (t or dd, $^3J(P-H_A)$ = $^2J(H_A-H_x)$ = 10.6 Hz, 2 H, $OCH_2(A)$), 5.32 (impurity), 6.42–7.60 (m, 6 H, H_{aryl}), 9.05 (d, $^2J(P-H)$ = 27 Hz, 1 H, N*H*). ^{31}P NMR ($CDCl_3$, ppm): −58.84. Anal. Calcd for $C_{18}H_{23}O_4N_2P$: C, 59.66; H, 6.40; N, 7.73. Found: C, 59.47; H, 6.34; N, 7.72.

Reaction of 2-(2,6-Dimethylphenoxy)-5,5-dimethyl-1,3,2-dioxaphosphorinane with 2-Hydroxybenzyl Alcohol. Formation of 2,6-Dimethylphenyl 2,2-Dimethylpropylene Phosphate, ($Me_2C_3H_4O_2$)P(O)(O-Xyl) (3). 2-(2,6-Dimethylphenoxy)-5,5-dimethyl-1,3,2-dioxaphosphorinane (2.2 g, 8.7 mmol) was dissolved in diethyl ether (60 mL). 2-Hydroxybenzyl alcohol (1.0 g, 8.7 mmol) and *N*-chlorodiisopropylamine (1.17 g, 8.7 mmol) were added, and the mixture was stirred for 6 h. After filtration, hexane (1.5 mL) was added, and the solution was left at room temperature whereupon crystallization occurred. Concentration of the mother liquor gave a second fraction of crystals, mp 118–119 °C (1.6 g, 68%). ^1H NMR ($CDCl_3$, ppm): 0.96 (s, 3 H, OCH_2CH_3), 1.30 (s, 3 H, OCH_2CH_3), 2.33 (s, 6 H, $C_6H_3(CH_3)_2$), 4.11 (dd, $^3J(P-H_x)$ = 19.9 Hz, $^2J(H_A-H_x)$ = 11.0 Hz, 2 H, $OCH_2(X)$), 4.35 (dd, $^3J(P-H_A)$ = 4.4 Hz, $^2J(H_A-H_x)$ = 10.8 Hz, 2 H, $OCH_2(A)$), 6.93–7.04 (m, 3 H, H_{aryl}). ^{31}P NMR ($CDCl_3$, ppm): −14.5. Anal. Calcd for $C_{13}H_{19}O_4P$: C, 57.78; H, 7.09. Found: C, 57.93; H, 7.17.

2-(2,6-Dimethylphenoxy)-5,5',5',7-tetramethylspiro[1,3,2-benzoxazaphosphole-2(3*H*),2'λ⁵-[1,3,2]dioxaphosphorinane], ($Me_2C_3H_4O_2$)($Me_2C_6H_2ONH$)P(O-Xyl) (4). 2-Amino-4,6-dimethylphenol (1.24 g, 9.1 mmol) and 2-(2,6-dimethylphenoxy)-5,5-dimethyl-1,3,2-dioxaphosphorinane (2.3 g, 9.1 mmol) were suspended in diethyl ether (75 mL). *N*-Chlorodiisopropylamine (1.2 g, 9.1 mmol) was added with stirring. After 28 h the reaction mixture was filtered. Fractionated crystallization afforded a slightly yellow powder, mp 132 °C (1.1 g, 31%). ^1H NMR (CD_2Cl_2, ppm): 1.00 (s, 3 H, OCH_2CH_3), 1.20 (s, 3 H, OCH_2CH_3), 1.52 (s, 3 H, CH_{3para}), 2.16 (s, 3 H, CH_{3ortho}), 2.18 (s, 6 H, $C_6H_3(CH_3)_2$), 3.86 (dd, $^3J(P-H_x)$ = 21.3 Hz, $^2J(H_A-H_x)$ = 12.1 Hz, 2 H, $OCH_2(X)$), 4.24 (t or dd, $^3J(P-H_A)$ = $^2J(H_A-H_x)$ = 9.6 Hz, 2 H, $OCH_2(A)$), 5.32 (impurity), 5.60 (d, $^2J_{P-H}$ = 19.5 Hz, 1 H, N*H*), 6.25–6.91 (m, 5 H, H_{aryl}). ^{31}P NMR ($CDCl_3$, ppm): −56.88. Anal. Calcd for $C_{21}H_{28}O_4NP$: C, 64.76; H, 7.24; N, 3.59. Found: C, 64.51; H, 7.11; N, 3.58.

(15) van Ool, P. J. J. M.; Buck, H. M. *Recl. Trav. Chim. Pays-Bas* **1981**, *100*, 79.
(16) van Ool, P. J. J. M.; Buck, H. M. *Eur. J. Biochem.* **1982**, *121*, 329.
(17) Emsley, J.; Hall, D. *The Chemistry of Phosphorus*; Wiley: New York, 1976; p 82.

Table I. Crystallographic Data for Compounds **1**–**3**

compd	**1**	**2**	**3**
formula	$C_{19}H_{23}O_6N_2P$	$C_{18}H_{23}O_4N_2P$	$C_{13}H_{19}O_4P$
fw	406.38	362.37	270.27
cryst color	yellow-orange	colorless	colorless
cryst dimens, Å	0.38 × 0.50 × 0.55	0.07 × 0.33 × 0.60	0.40 × 0.49 × 0.49
cryst system	monoclinic	monoclinic	orthorhombic
space group	$P2_1/c$ (No. 14)	$P2_1/n$ (No. 14)	$P2_12_12_1$ (No. 19)
a, Å	8.1618 (9)	11.200 (2)	7.253 (1)
b, Å	20.240 (4)	27.347 (8)	9.456 (2)
c, Å	12.577 (1)	12.865 (3)	20.510 (3)
β, deg	103.26 (1)	105.23 (2)	
V, Å^3	2022.3	3802	1406.7
Z	4	8	4
D_{calc}, g/cm^3	1.335	1.266	1.276
μ, cm^{-1}	1.664	1.620	1.926
rel transm coeff	0.9589–1.000	0.9409–0.9986	
no. of independ data ($+h,+k,\pm l$)	3539	4345	1452
no. of obsd data ($I \geq 3\sigma_I$)	2511	2021	1203
$R(F)$	0.037	0.050	0.035
$R_w(F)$	0.051	0.062	0.047

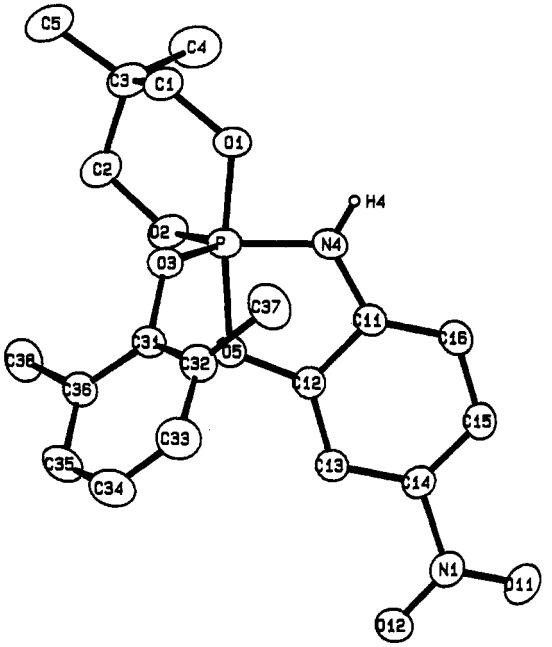

Figure 1. ORTEP plot of $(Me_2C_3H_4O_2)(O_2NC_6H_3ONH)P(O\text{-}Xyl)$ (**1**) with thermal ellipsoids at the 30% probability level. Hydrogen atoms, except for H4, are omitted for clarity.

Attempts were made to grow crystals for an X-ray analysis but apparently ready loss of solvent caused the crystals to become powdery as observed under the microscope and during data collection.

X-ray Experimental Section

All X-ray crystallographic studies were done by using an Enraf-Nonius CAD4 diffractometer and graphite-monochromated molybdenum radiation ($\lambda(K\bar{\alpha})$ = 0.710 73 Å) at an ambient temperature of 23 ● 2 °C. Details of the experimental procedures have been described previously.[18] Crystals were mounted in thin-walled glass capillaries, which were sealed as a precaution against moisture sensitivity. Data were collected by using the θ–2θ scan mode with $3° \leq 2\theta(\text{Mo } K\bar{\alpha}) \leq 50°$ for **1** and **3** and $3° \leq 2\theta(\text{Mo } K\bar{\alpha}) \leq 43°$ for **2**. The structures were solved by use of direct methods and difference Fourier techniques and were refined by full-matrix least squares.[19]

Non-hydrogen atoms were refined anisotropically, while amino hydrogen atoms were refined isotropically. The remaining hydrogen atoms were included in the refinements as fixed isotropic scatterers (ideal positions or regularized difference Fourier positions for the xylyl methyl groups).

For **2**, large isotropic thermal parameters for C22, C24, and C25 suggested disorder but attempts to resolve two positions for atom C22 were unsuccessful. Two sets of positions were obtained for C24 and C25, which were included in the refinement in partial occupancy on the basis of relative electron density (0.56 for A, 0.44 for B).

All computations were performed on a Microvax II computer using the Enraf-Nonius SDP system of programs. Crystallographic data are summarized in Table I.[20]

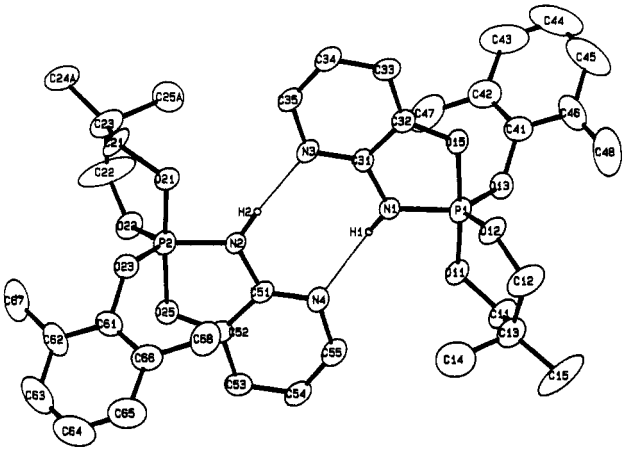

Figure 2. ORTEP plot showing the asymmetric unit in $(Me_2C_3H_4O_2)(C_5H_3NONH)P(O\text{-}Xyl)$ (**2**) with thermal ellipsoids at the 30% probability level. All but the amino hydrogen atoms are omitted for clarity. Hydrogen bonds are shown as narrow lines. Only one set of positions for the disordered C24 and C25 is shown.

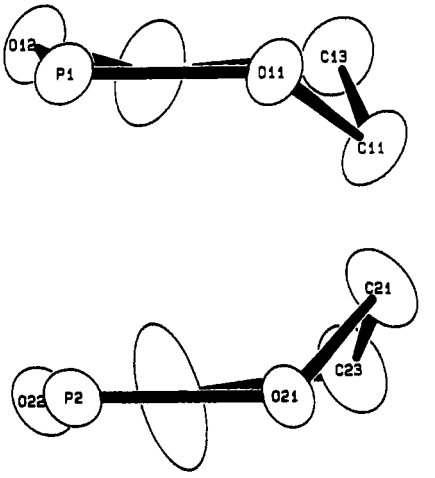

Figure 3. ORTEP plots showing the conformations of the phosphorinane ring systems in $(Me_2C_3H_4O_2)(C_5H_3NONH)P(O\text{-}Xyl)$ (**2**).

(18) Sau, A. C.; Day, R. O.; Holmes, R. R. *Inorg. Chem.* **1981**, *20*, 3076.
(19) The function minimized was $\sum w(|F_o| - |F_c|)^2$, where $w^{1/2} = 2F_oLp/\sigma_I$.
(20) $R = \sum||F_o| - |F_c||/\sum|F_o|$ and $R_w = [\sum w(|F_o| - |F_c|)^2/\sum w|F_o|^2]^{1/2}$. For **3**, these values are for the configuration with the lowest R_w.

Table II. Selected Distances (Å) and Angles (deg) for $(Me_2C_3H_4O_2)(O_2NC_6H_3ONH)P(O\text{-}Xyl)$ (**1**)[a]

		Distances	
P–O1	1.646 (2)	O11–N1	1.216 (3)
P–O2	1.583 (2)	O12–N1	1.215 (3)
P–O3	1.607 (2)	N1–C14	1.457 (3)
P–O5	1.751 (2)	N4–C11	1.375 (3)
P–N4	1.667 (2)	C1–C3	1.519 (3)
O1–C1	1.425 (3)	C2–C3	1.507 (4)
O2–C2	1.454 (3)	C3–C4	1.528 (4)
O3–C31	1.404 (3)	C3–C5	1.533 (4)
O5–C12	1.343 (2)	N4–H4	0.78 (2)
N4–O12′	2.948 (3)	H4–O12′	2.21 (2)
		Angles	
O1–P–O2	98.65 (8)	P–O3–C31	128.6 (1)
O1–P–O3	91.56 (8)	P–O5–C12	114.5 (1)
O1–P–O5	172.02 (8)	O11–N1–O12	121.8 (2)
O1–P–N4	85.86 (9)	O11–N1–C14	119.5 (2)
O2–P–O3	111.14 (8)	O12–N1–C14	118.7 (2)
O2–P–O5	86.93 (8)	P–N4–C11	118.3 (2)
O2–P–N4	123.72 (9)	O1–C1–C3	110.2 (2)
O3–P–O5	91.73 (8)	O2–C2–C3	113.8 (2)
O3–P–N4	124.85 (9)	C1–C3–C2	106.9 (2)
O5–P–N4	86.30 (8)	P–N4–H4	119 (2)
P–O1–C1	123.1 (1)	C11–N4–H4	122 (2)
P–O2–C2	122.8 (1)	N4–H4–O12′	156 (2)

[a] Estimated standard deviations in parentheses. The atom-labeling scheme is shown in Figure 1.

Table III. Selected Distances (Å) and Angles (deg) for $(Me_2C_3H_4O_2)(C_5H_3NONH)P(O\text{-}Xyl)$ (**2**)[a]

		Distances	
P1–O11	1.633 (5)	O11–C11	1.431 (8)
P1–O12	1.587 (4)	O12–C12	1.420 (8)
P1–O13	1.603 (5)	O21–C21	1.456 (8)
P1–O15	1.752 (5)	O22–C22	1.400 (9)
P1–N1	1.656 (5)	C11–C13	1.501 (9)
P2–O21	1.640 (5)	C12–C13	1.49 (1)
P2–O22	1.594 (4)	C21–C23	1.549 (9)
P2–O23	1.601 (4)	C22–C23	1.43 (1)
P2–O25	1.752 (5)	N1–H1	0.82 (6)
P2–N2	1.663 (5)	N2–H2	0.91 (6)
H1–N4	2.08 (6)	H2–N3	2.01 (6)
		Angles	
O11–P1–O12	98.1 (2)	O23–P2–N2	123.7 (2)
O11–P1–O13	90.7 (2)	O25–P2–N2	87.9 (2)
O11–P1–O15	174.5 (2)	P1–O11–C11	122.7 (4)
O11–P1–N1	87.4 (3)	P1–O12–C12	129.5 (5)
O12–P1–O13	114.5 (2)	P2–O21–C21	119.8 (4)
O12–P1–O15	86.7 (2)	P2–O22–C22	128.6 (6)
O12–P1–N1	121.1 (3)	O11–C11–C13	109.0 (6)
O13–P1–O15	89.8 (2)	O12–C12–C13	116.3 (6)
O13–P1–N1	124.0 (2)	C11–C13–C12	108.8 (6)
O15–P1–N1	87.8 (2)	O21–C21–C23	106.8 (6)
O21–P2–O22	97.9 (2)	O22–C22–C23	123.4 (7)
O21–P2–O23	90.4 (2)	C21–C23–C22	110.9 (6)
O21–P2–O25	175.8 (2)	P1–N1–C31	117.0 (4)
O21–P2–N2	88.1 (2)	P1–N1–H1	127 (5)
O22–P2–O23	115.0 (2)	C31–N1–H1	116 (5)
O22–P2–O25	85.3 (2)	P2–N2–C51	117.1 (4)
O22–P2–N2	121.0 (3)	P2–N2–H2	124 (4)
O23–P2–O25	90.7 (2)	C51–N2–H2	118 (4)
P1–O13–C41	128.8 (4)	P2–O23–C61	129.2 (4)
P1–O15–C32	113.4 (4)	P2–O25–C52	113.2 (4)
N1–H1–N4	170 (6)	N2–H2–N3	167 (5)

[a] Estimated standard deviations in parentheses. The atom-labeling scheme is shown in Figure 2.

Results

X-ray Studies. The atom-labeling scheme for **1** is given in the ORTEP plot of Figure 1, while selected bond lengths and angles are given in Table II. The corresponding information for **2** and **3** appears in Figures 2 and 4 and in Tables III and IV, respectively. Atomic coordinates are given in Tables V–VII. For all three compounds, anisotropic thermal parameters, additional bond lengths and angles, and hydrogen atom parameters are provided as supplementary material.

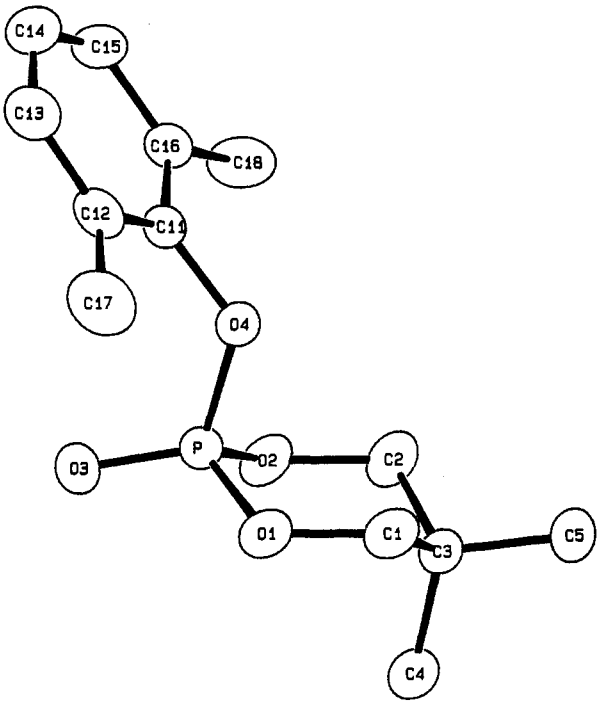

Figure 4. ORTEP plot of $(Me_2C_3H_4O_2)P(O)(O\text{-}Xyl)$ (**3**) with thermal ellipsoids at the 30% probability level. Hydrogen atoms are omitted for clarity.

Table IV. Selected Distances (Å) and Angles (deg) for $(Me_2C_3H_4O_2)P(O)(O\text{-}Xyl)$ (**3**)[a]

		Distances	
P–O1	1.565 (2)	O1–C1	1.451 (4)
P–O2	1.560 (2)	O2–C2	1.455 (4)
P–O3	1.448 (3)	C1–C3	1.521 (4)
P–O4	1.582 (2)	C2–C3	1.513 (4)
		Angles	
O1–P–O2	104.4 (1)	P–O1–C1	118.3 (2)
O1–P–O3	113.9 (1)	P–O2–C2	118.2 (2)
O1–P–O4	102.9 (1)	O1–C1–C3	112.0 (2)
O2–P–O3	113.3 (1)	O2–C2–C3	111.6 (2)
O2–P–O4	105.3 (1)	C1–C3–C2	108.7 (2)
O3–P–O4	115.8 (1)	P–O4–C11	125.4 (2)

[a] Estimated standard deviations in parentheses. The atom-labeling scheme is shown in Figure 4.

Table V. Selected Atomic Coordinates and B_{eq} Values (Å^2) in Crystalline $(Me_2C_3H_4O_2)(O_2NC_6H_3ONH)P(O\text{-}Xyl)$ (**1**)[a]

atom[b]	x	y	z	B_{eq}[c]
P	0.23332 (7)	0.14208 (3)	0.73056 (5)	3.40 (1)
O1	0.0271 (2)	0.14293 (8)	0.7143 (1)	3.95 (3)
O2	0.2761 (2)	0.20831 (8)	0.7986 (1)	4.12 (3)
O3	0.2172 (2)	0.15504 (7)	0.6024 (1)	3.58 (3)
O5	0.4511 (2)	0.12956 (7)	0.7527 (1)	3.69 (3)
N4	0.2261 (2)	0.06781 (9)	0.7872 (2)	4.09 (4)
C1	−0.0721 (3)	0.2013 (1)	0.6883 (2)	4.27 (5)
C2	0.1705 (3)	0.2670 (1)	0.7772 (2)	4.56 (6)
C3	−0.0125 (3)	0.2541 (1)	0.7745 (2)	4.51 (5)
C4	−0.0357 (4)	0.2308 (2)	0.8858 (2)	6.67 (8)
C5	−0.1091 (4)	0.3188 (2)	0.7412 (3)	6.35 (8)
C11	0.3737 (3)	0.0326 (1)	0.8189 (2)	3.42 (4)
C12	0.5047 (3)	0.0707 (1)	0.7970 (2)	3.26 (4)
C31	0.3362 (3)	0.1427 (1)	0.5397 (2)	3.38 (4)

[a] Numbers in parentheses are estimated standard deviations. [b] Atoms are labeled to agree with Figure 1. [c] Equivalent isotropic thermal parameters are calculated as $(4/3)[a^2\beta_{11} + b^2\beta_{22} + c^2\beta_{33} + ab(\cos\gamma)\beta_{12} + ac(\cos\beta)\beta_{13} + bc(\cos\alpha)\beta_{23}]$.

NMR Studies. Analysis of variable-temperature ^{1}H NMR spectra yielded activation energies, $\Delta G^{\ddagger}$,[21] that are reported in

Table VI. Selected Atomic Coordinates and B_{eq} Values (Å^2) in Crystalline $(Me_2C_3H_4O_2)(C_5H_3NONH)P(O\text{-}Xyl)$ (**2**)[a]

atom[b]	x	y	z	B_{eq}[c]
P1	0.0331 (2)	0.13887 (7)	0.7323 (1)	3.95 (4)
P2	-0.0183 (2)	0.35452 (7)	1.0082 (1)	3.79 (4)
O11	0.0831 (4)	0.1786 (2)	0.6588 (3)	4.1 (1)
O12	-0.0816 (4)	0.1188 (2)	0.6420 (3)	4.7 (1)
O13	0.1572 (4)	0.1074 (2)	0.7480 (3)	4.3 (1)
O15	-0.0149 (4)	0.0999 (2)	0.8217 (3)	4.1 (1)
O21	-0.0620 (4)	0.3148 (2)	1.0865 (3)	4.0 (1)
O22	0.0936 (4)	0.3784 (2)	1.0965 (3)	4.5 (1)
O23	-0.1477 (4)	0.3826 (2)	0.9893 (3)	4.0 (1)
O25	0.0265 (4)	0.3935 (2)	0.9172 (3)	4.2 (1)
N1	0.0174 (5)	0.1850 (2)	0.8111 (4)	4.0 (1)
N2	0.0050 (5)	0.3078 (2)	0.9330 (4)	4.0 (1)
N3	-0.0362 (5)	0.2056 (2)	0.9729 (4)	4.1 (1)
N4	0.0631 (5)	0.2868 (2)	0.7731 (4)	4.3 (1)
C11	0.0820 (6)	0.1695 (3)	0.5491 (5)	5.0 (2)
C12	-0.1049 (7)	0.1208 (3)	0.5281 (6)	7.6 (2)
C13	-0.0494 (6)	0.1631 (3)	0.4837 (5)	5.5 (2)
C14	-0.1267 (9)	0.2094 (4)	0.4913 (8)	9.1 (3)
C15	-0.0542 (9)	0.1519 (5)	0.3664 (6)	11.6 (4)
C21	-0.0669 (6)	0.3293 (3)	1.1942 (5)	5.2 (2)
C22	0.1337 (9)	0.3681 (5)	1.2069 (7)	12.3 (3)
C23	0.0686 (7)	0.3366 (3)	1.2613 (5)	6.2 (2)
C24A	0.077 (1)	0.3434 (5)	1.379 (1)	7.4 (4)
C24B	0.057 (2)	0.3881 (7)	1.339 (1)	7.6 (5)
C25A	0.153 (1)	0.2871 (5)	1.249 (1)	6.5 (4)
C25B	0.106 (2)	0.2966 (8)	1.339 (2)	10.5 (6)
C31	-0.0203 (6)	0.1738 (2)	0.9007 (5)	3.4 (2)
C32	-0.0385 (5)	0.1236 (2)	0.9066 (5)	3.5 (2)
C33	-0.0769 (6)	0.1040 (2)	0.9905 (5)	4.4 (2)
C34	-0.0949 (6)	0.1370 (3)	1.0675 (5)	4.7 (2)
C35	-0.0753 (7)	0.1868 (3)	1.0569 (5)	4.8 (2)
C41	0.1989 (6)	0.0683 (3)	0.8175 (5)	5.0 (2)
C51	0.0426 (6)	0.3189 (2)	0.8416 (5)	3.4 (2)
C52	0.0523 (5)	0.3697 (2)	0.8342 (5)	3.7 (2)
C53	0.0867 (6)	0.3888 (2)	0.7477 (5)	4.3 (2)
C54	0.1082 (6)	0.3549 (3)	0.6727 (5)	4.9 (2)
C55	0.0960 (6)	0.3070 (3)	0.6873 (5)	5.0 (2)
C61	-0.1960 (6)	0.4213 (3)	0.9171 (5)	4.5 (2)

[a] Numbers in parentheses are estimated standard deviations. [b] Atoms are labeled to agree with Figure 2. [c] See footnote *c* of Table V.

Table VII. Selected Atomic Coordinates and B_{eq} Values (Å^2) in Crystalline $(Me_2C_3H_4O_2)P(O)(O\text{-}Xyl)$ (**3**)[a]

atom[b]	x	y	z	B_{eq}[c]
P	0.5747 (1)	0.95963 (9)	0.85494 (4)	3.83 (1)
O1	0.5766 (3)	1.0797 (3)	0.8025 (1)	4.71 (4)
O2	0.3977 (3)	0.8723 (2)	0.8392 (1)	4.45 (5)
O3	0.7410 (3)	0.8749 (3)	0.8560 (1)	6.28 (6)
O4	0.5289 (3)	1.0424 (2)	0.92002 (9)	3.81 (4)
C1	0.4062 (5)	1.1552 (3)	0.7896 (2)	4.67 (7)
C2	0.2271 (4)	0.9488 (4)	0.8269 (2)	4.94 (7)
C3	0.2494 (4)	1.0552 (3)	0.7724 (1)	3.74 (6)
C4	0.2866 (5)	0.9840 (4)	0.7072 (2)	5.21 (8)
C5	0.0730 (5)	1.1450 (4)	0.7678 (2)	6.52 (9)
C11	0.6079 (4)	1.0150 (3)	0.9816 (1)	3.54 (6)

[a] Numbers in parentheses are estimated standard deviations. [b] Atoms are labeled to agree with Figure 4. [c] See footnote *c* of Table V.

Table VIII. Activation Parameters of Ligand Exchange Determined from Variable-Temperature ^{1}H NMR Spectra

compd	temp range, °C	T_c, °C	$\Delta\nu$, Hz	$\Delta G_c^{\ddagger}$,[a] kcal/mol
1	-90 to +18	-42	249	10.5[b]
1	-90 to +18	-35	90	11.3[c]
2	-63 to +18	-8.1	106.4	12.6[c]
2	-63 to +18	-28	202.6	11.3[b]
4	-68 to +20	-9	75	12.5[c]
4	-68 to +20	-28	244	11.2[b]

[a] Values are estimated to be accurate to within ±1.5 kcal/mol. See ref 21. [b] $\Delta G^{\ddagger}$ calculated from coalescence of $C_6H_3(CH_3)_2$ signals. [c] $\Delta G^{\ddagger}$ calculated from coalescence of OCH_2 signals.

Table VIII along with the coalescence temperatures (T_c) and line separations ($\Delta\nu$) used in the calculations.

Discussion

Synthesis and Basic Structures. All three new tetraoxyphosphoranes, **1**, **2**, and **4**, were formed by oxidative addition of an *o*-aminophenol to the monocyclic phosphite **5** at room temperature in either diethyl ether or tetrahydrofuran solution (eq 1). When 2-hydroxybenzyl alcohol was used as the reactant with

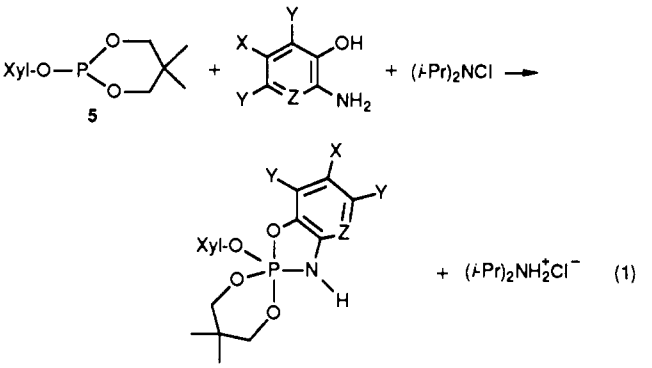

1 (X = NO_2, Y = H, Z = CH)
2 (X = Y = H, Z = N)
4 (X = H, Y = Me, Z = CH)

5 in eq 1, phosphate **3** formed instead of the expected phosphorane. A hydrolysis reaction of **5** was suspected; however, the yield of **3** was 68%. To decide the issue, the reaction was conducted under identical conditions but in the absence of the alcohol. No reaction occurred implying that an oxo addition took place in the presence of the alcohol to give the phosphate, **3**. If we balance the reaction, either $(-OC_6H_4CH_2-)_n$ or benzoxetane appears as a likely product (eq 2).

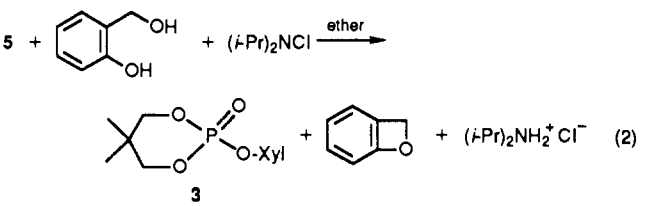

3

Intermolecular N–H---O hydrogen bonding gives rise to a chain structure for **1**. For **2** N–H---N hydrogen bonding exists that provides a dimeric unit. The geometry about the phosphorus atoms in **1** and **2** can be referred to a trigonal bipyramid with the ring systems spanning axial–equatorial sites and the nitrogen atom in an equatorial position. For all three phosphorus centers, distortions away from the trigonal bipyramid do not follow the Berry pseudorotation coordinate[22] but are "anti-Berry" in nature. In all cases the O_{eq}–P–O_{eq} is smaller than 120° (111.14 (8), 114.5 (2), 115.0 (2)°), while the axial oxygen atoms are tipped toward the equatorial nitrogen atom (O_{ax}–P–O_{ax} = 172.02 (8), 174.5 (2), and 175.8 (2)° for **1** and P1 and P2 of **2**, respectively).

The five-membered rings in **1** and **2** are essentially planar and are coplanar with the fused six-membered rings. For **1**, the nine atoms P, N4, O5, and C11–C16 are coplanar to within ±0.020 Å. For **2**, the correspondings values are ±0.006 and ±0.023 Å for the molecules containing P1 and P2, respectively. In addition, for **2**, the two nine-atom planes are close to coplanar with a dihedral angle between them of 3.5°.

The phosphate **3** gives the expected tetrahedral structure with the phosphorinane ring in a chair conformation. It is noted that although the chair conformation is the common one for phosphates containing saturated six-membered rings, there is an abundance of related tetracoordinate phosphorus compounds containing dithiaphosphorinane rings that have these rings in a twist-boat conformation.[23]

(21) Calculated from the equation $\Delta G_c^{\ddagger} = 4.57 \times 10^{-3} T_c(10.32 + \log(T_c\sqrt{2}/\pi\Delta\nu))$ following: Kessler, H. *Angew. Chem.* **1970**, *82*, 237. See also: Buono, G.; Llinas, J. R. *J. Am. Chem. Soc.* **1981**, *103*, 4532.
(22) Berry, R. S. *J. Chem. Phys.* **1960**, *32*, 933.
(23) Maryanoff, B. E.; Hutchins, R. O.; Maryanoff, C. A. *Top. Stereochem.* **1979**, *11*, 187 and references cited therein.

Table IX. Comparison of Ring and Acyclic P–O Bond Lengths (Å) for Phosphoranes **1**, **2**, and A–C

compd	six-membered ring		five-membered ring	acyclic
	$P–O_{ax}$	$P–O_{eq}$	$P–O_{ax}$	$P–O_{eq}$
1[a]	1.646	1.583	1.751	1.607
2[b]	1.633	1.587	1.752	1.603
2[c]	1.640	1.594	1.752	1.601
1, **2**(av)[d]	1.640	1.588	1.752	1.604
A–C(av)[e,f]	1.648[h]	1.595	1.714	1.610
A–C(av)[g,f]	1.672	1.586[h]	1.740[h]	

[a] Chair for phosphorinane ring. [b] Twist-chair of half-chair for phosphorinane ring containing P1. [c] Phosphorinane ring containing P2 has disorder at C22. [d] Averages of values for **1** and **2**. [e] Averages of values for non-hydrogen-bonded bond lengths of A–C. [f] From ref 12. [g] Average of values for hydrogen-bonded bond lengths of A–C. [h] Represents a single value.

Intermolecular Hydrogen Bonding. Unlike the previous structures A–C,[12] which have both hydrogen bonding and the phosphorinane ring system similar to those of **1** and **2** in the present study, the oxygen atoms of the rings of the latter compounds are not involved in hydrogen bonding. In **1**, the amino hydrogen atoms, H4, form hydrogen-bonding interactions with the nitro oxygen atoms, O12, of translationally related molecules, giving hydrogen-bonded chains along *a*. In **2** the asymmetric unit consists of a pair of crystallographically independent molecules that are joined by a pair of N–H···N hydrogen bonds to form a hydrogen-bonded dimer. The symmetry of the dimer thus formed is approximately C_i.

It is reasonable that the monocoordinated oxygen atoms of the nitro group in **1** form hydrogen bonds in preference to hydrogen-bond formation involving bicoordinated ring oxygen atoms. While the N–H···O hydrogen-bond distances for **1** and those of the related phosphoranes B and C[12] do not differ significantly, the downfield chemical shifts assigned to the N–H proton suggest an order of donor strength pyridine (**2**) > nitro (**1**) > ring oxygens (A–C and **4**). The respective N–H proton chemical shifts in ppm are 9.1 (**2**), 6.24 (**1**), 5.60 (**4**), and 5.29 (average of A–C[12]). For A,[12] the NH group enters into a bifurcated hydrogen bond with two ring oxygen atoms. As a consequence, the N–H···O distances are appreciably longer (3.24 and 3.20 Å) than those for **1**, B, and C (2.93 ± 0.03 Å average).

The stronger donor N–H hydrogen bonds implied for **1** and **2** compared to those in A–C are in accord with the longer $P–O_{ax}$ bond lengths for the five-membered rings of **1** and **2**. They average 1.752 ± 0.003 Å (Table IX) compared with 1.714 ± 0.003 Å for the average values of A–C. An enhancement of the electron-withdrawing capacity due to the presence of the nitrophenyl and pyridine moieties should result in a weakened P–O axial bond. In complimentary fashion, the opposite $P–O_{ax}$ bond lengths of the six-membered rings lacking any hydrogen bonding in **1** and **2** are shorter, 1.640 ± 0.004 Å (Table IX), than the $P–O_{ax}$ bond lengths of the corresponding rings of A–C that are involved in hydrogen bonding, 1.672 ± 0.003 Å (Table IX).

If **1** were to exist as a dimer like **2**, a 16 atom hydrogen-bonded ring would form. While somewhat unique,[24] this would bring the two nitrophenyl groups into steric interference with each other, i.e., under the logical assumption that the whole unit would be essentially planar. The dimeric arrangement for **2** has an eight-membered hydrogen-bonded ring with little steric hindrance between the two participating molecules.

Phosphorinane Ring Conformations. The conformation of the phosphorinane rings in **1** and **3** is best described as a chair that is somewhat flattened at the phosphorus end (Figure 5, top and bottom). For **3**, the atoms O1, O2, C1, and C2 are essentially coplanar (±0.003 (3) Å) with atoms P and C3 displaced in opposite directions from this plane by 0.606 (1) and 0.683 (3) Å,

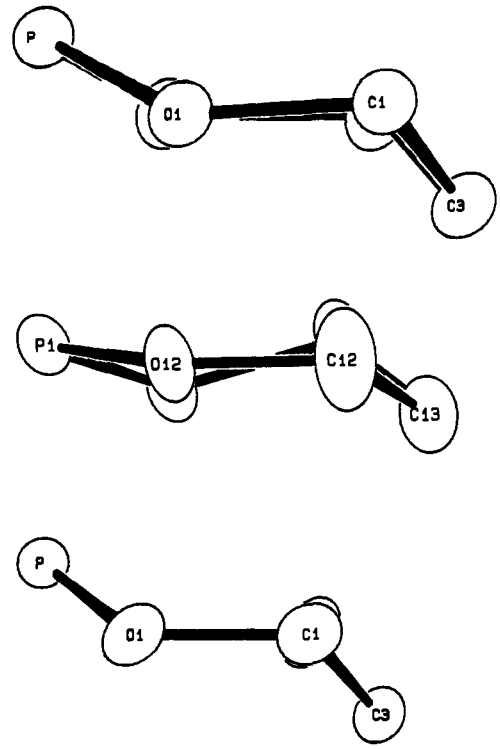

Figure 5. ORTEP plots comparing the conformations of the phosphorinane ring systems in **1** (top), **2** (middle), and **3** (bottom).

respectively. The dihedral angles between this plane and the three atom planes defined by P or C3 and their two nearest neighbors are 39.3 (2) and 50.6 (3)°, respectively. For **1**, where the distortions are somewhat more pronounced, the corresponding values are ±0.020 (2) Å, 0.566 (1) Å, 0.706 (2) Å, 32.5 (1)°, and 51.6 (2)°.

The geometry of the phosphorinane ring in **2** appears, when viewed in a corresponding way, as a very twisted chair (Figure 5, middle) and is perhaps closest to a half-chair (Figure 3). For the molecule containing P1, the best four-atom plane is defined by P1, O11, C12, and C13 (±0.034 Å). Atoms O12 and C11 are displaced in opposite directions from this plane by 0.247 and 0.674 Å, respectively. The best four-atom plane defined by four adjacent atoms is the one through O11, P1, O12, and C12 (±0.097 Å). Atoms C13 and C11 are displaced in opposite directions from this plane by 0.171 and 0.506 Å, respectively. For the molecule containing P2, the conformation appears to be similar (Figure 3) but the details of the geometry are suspect due to the disorder in that portion of the molecule.

We see that the phosphorinane ring system takes on the chair conformation rather than the boat conformation in phosphoranes A–C and **1** and **2** that possess N–H hydrogen-bonding features. The only other example of a phosphorane that has a chair conformation for this same ring system is in the pentafluorophenyl derivative, D, described in the Introduction, where steric and electronegative considerations have been cited[1b] as contributing factors for its formation.

As discussed earlier in connection with the phosphorinane conformations of A–C,[12] axial and equatorial P–O bond lengths do not show significant differences between chair and boat conformations for phosphoranes to warrant their use to differentiate between these forms.[25] Apparently, the presence of hydrogen bonding by allowing the formation of chain and dimer structures reduces the relatively small energy difference[12] between the two conformations, perhaps via mild steric interactions that may arise as a result of the formation of these structural arrangements. Steric effects certainly seem to be a possibility in contributing to the presence of the chair conformation for D.[1b]

(24) Poutasse, C. A.; Day, R. O.; Holmes, R. R. *J. Am. Chem. Soc.* **1984**, *106*, 3814.

(25) Compare bond lengths in Table IX here with Table VII of ref 12 and Table X of ref 7.

Table X. Dihedral Angles between P–O_{eq}–C Planes and Equatorial Planes for Spirocyclic Phosphoranes (deg)

compd	ring size, no. of atoms: 5	ring size, no. of atoms: 6	xylyloxy group	phosphorinane conformation
1[a]	89.2	54.8	77.0	chair
2[a]	88.7	70.9	85.7	twist-chair[c]
2[a]	87.9		87.7	*d*
A[b]	88.2	72.5	89.8	twist-chair
B[b]	83.8	64.1	89.0	twist-boat
B[b]	87.8	63.9	74.5	twist-chair
C[b]	90.0	67.1	86.4	twist-boat
C[b]	89.7	63.4/67.9	85.3	twist-boat/chair[d]
av	88.2	65.6 ± 4.0	84.4	

[a] This work. Rings do not have oxygen atoms hydrogen bonded. [b] Reference 12. Rings have oxygen atoms hydrogen bonded. [c] Or half-chair. [d] Disordered ring.

In any event, the introduction of hydrogen bonding produces some common structural features that are independent of whether a boat or chair form exists compared to the presence of the normally observed boat conformation in phosphoranes without hydrogen bonding. As shown in Table X, the dihedral angles between endocyclic P–O_{eq}–C planes and equatorial planes for the six-membered rings of phosphoranes that exhibit hydrogen bonding are in a lower range (average 65.6°) relative to these dihedral angles for other groups. The dihedral angles for these latter groups tend toward 90°, the angle that Trippett[11] predicted for the best positioning of lone pairs on the oxygen atom of the P–O_{eq} bond. For D,[1b] a low dihedral angle (associated with the phosphorinane ring having a chair conformation) of 54.6° is found, similar to that in **1**. The average value of this dihedral angle for phosphorinane rings, independent of whether they are in boat or chair forms, for hydrogen-bonded phosphoranes is 65.6 ± 4.0°, which compares with 81.7 ± 3.8° for phosphorinane rings having boat conformations in phosphoranes without hydrogen bonding.[7,12] The lower values of the dihedral angles for the hydrogen-bonded systems relate to the form of the chair and twist-chair found for **1** and **2**, respectively, which has the part of the chair, atoms O1 and C1 (Figures 1 and 5, top, for **1**) and atoms O11 and C11 (Figures 3 and 5, middle, for **2**), tipped toward the xylyloxy group and away from the NH group. This is similar to that encountered with A–C, where it is concluded that this arrangement is most likely necessary to avoid steric interactions in the formation of the hydrogen-bonded species.[12] In all phosphorane compounds lacking hydrogen-bonding interactions, the phosphorinane rings in boat conformations are positioned such that the four-atom base of the boat is tipped away from the xylyloxy group. These ring conformations are illustrated in Figure 6. The torsion angle X–P–O_A–C_A defined in Figure 6 provides a measure of which ring form is present. Hydrogen-bonded phosphoranes like A–C, which have chair and boat ring conformations, have values of this angle in the range 151–169°,[12] whereas phosphoranes lacking hydrogen-bonding interactions show boat forms with torsion angles less than 69°.[26] The value of this angle is 165.6 (2)° for **1** and 159.2 (5)° (P1) and 163.0 (5)° (P2) for **2**. Thus consistency is provided among the hydrogen-bonded phosphoranes thus far studied and lends support for the formation of the associated conformations, Figure 6a,b, in providing a lower energy steric path leading to chain and dimer structures.

However, these solid-state considerations do not necessarily apply in solution. For **1**, **2**, and **4**, the NMR signal assigned to the NH proton moves progressively downfield on cooling the samples. Interpretation of the variable-temperature ^{1}H NMR data discussed in a following section indicates that the basic molecular structure observed in the solid state is retained in solution. At low temperatures a hydrogen-bonded chain for **1** and a dimer structure for **2** may be present whose percentage decreases relative to non-hydrogen-bonded structures as the temperature is increased. In the resulting monomer forms, the phosphorinane

(26) A more lengthy discussion is given in ref 12.

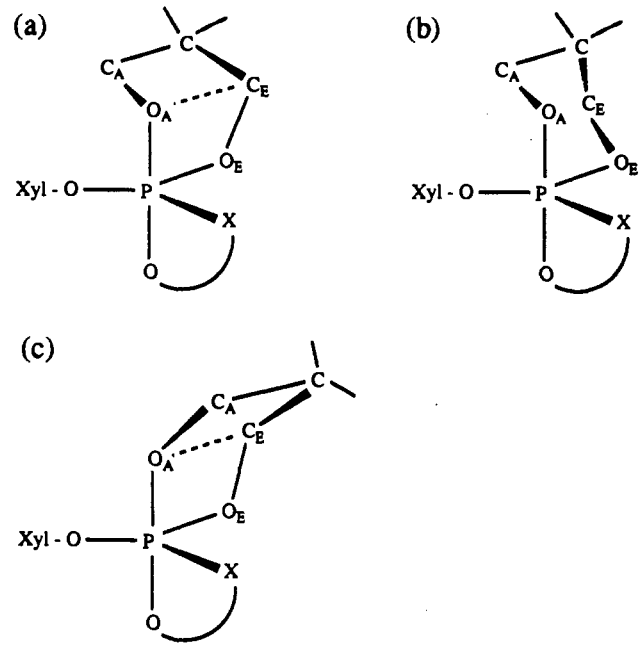

Figure 6. (a) Twist-boat as found in B[12] and C[12] (X = NH). The fold is along a line between "prow" atoms O_A and C_E such that C_A is away from X, with the torsion angle X–P–O_A–C_A > 90°. (b) Chair as in **1** and twist-chair as found in **2** and A–C.[12] This conformation can be converted to a twist-boat by moving only atom C_E into a prow position. The torsion angle X–P–O_A–C_A is essentially unchanged (>90°). (c) Boat as found in spirocyclic oxyphosphoranes[4,6,7] in the absence of hydrogen bonding (X = O). The fold along the line between "prow" atoms O_A and C_E is such that C_A is toward X, with the torsion angle X–P–O_A–C_A < 90°.

ring conformations may very well be exclusively in boat forms similar to that in Figure 6c. Although the ring conformation may change, the NMR evidence suggests that ring positioning at axial–equatorial sites of TBP structures is maintained in the ground-state representations.

Comparison of Chair Conformations in 1 and 3. Since the phosphorinane rings in **1** and **3** have similar conformations, it is of interest to compare their geometries in order to examine the effect of the coordination geometry at phosphorus.[27] In **3**, the phosphorinane ring and directly bonded atoms have pseudo-C_s symmetry with atoms P, O3, O4, C3, C4, and C5 (coplanar to within ±0.017 Å) lying on the pseudo mirror plane. Concomitant with this pseudosymmetry, the P–O bond lengths within the ring are within 3σ of each other (1.565 (2), 1.560 (2) Å). In the phosphorane **1**, the P–O_{ax} bond within the ring (1.646 (2) Å) is longer than the P–O_{eq} bond (1.585 (2) Å), and both distances are longer than those in **3** in keeping with the higher coordination number in **1**. In **1**, the O1–P–O2 bond angle (98.65 (8)°) is considerably less than the tetrahedral value and reflects the axial–equatorial placement of the ring. In **3** this value is more nearly tetrahedral (104.4 (1)°). There is also a noticeable difference in the P–O–C angles, which are nearly 5° smaller in **3** than in **1**.

NMR and Intramolecular Ligand Exchange. ^{31}P chemical shifts for **1**, **2**, and **4** in the range −57 to −59 ppm establish that the compounds remain pentacoordinated in solution. Figure 7 illustrates the variable-temperature ^{1}H NMR spectra for **2** in CD_2Cl_2 solution indicating intramolecular ligand exchange. Proceeding from right to left, the spectrum at 18.5 °C shows the phosphorinane ring methyl groups as two separate lines, the singlet signal for the xylyloxy methyls, two multiplets arising from the methylene protons of the six-membered ring that are composed of a higher field quartet and a lower field 1:2:1 triplet, an impurity signal, a number of peaks in the aromatic proton region, and a

(27) X-ray structures of less related tetracoordinated phosphates with saturated six-membered rings are found in the extensive summary listed in ref 23.

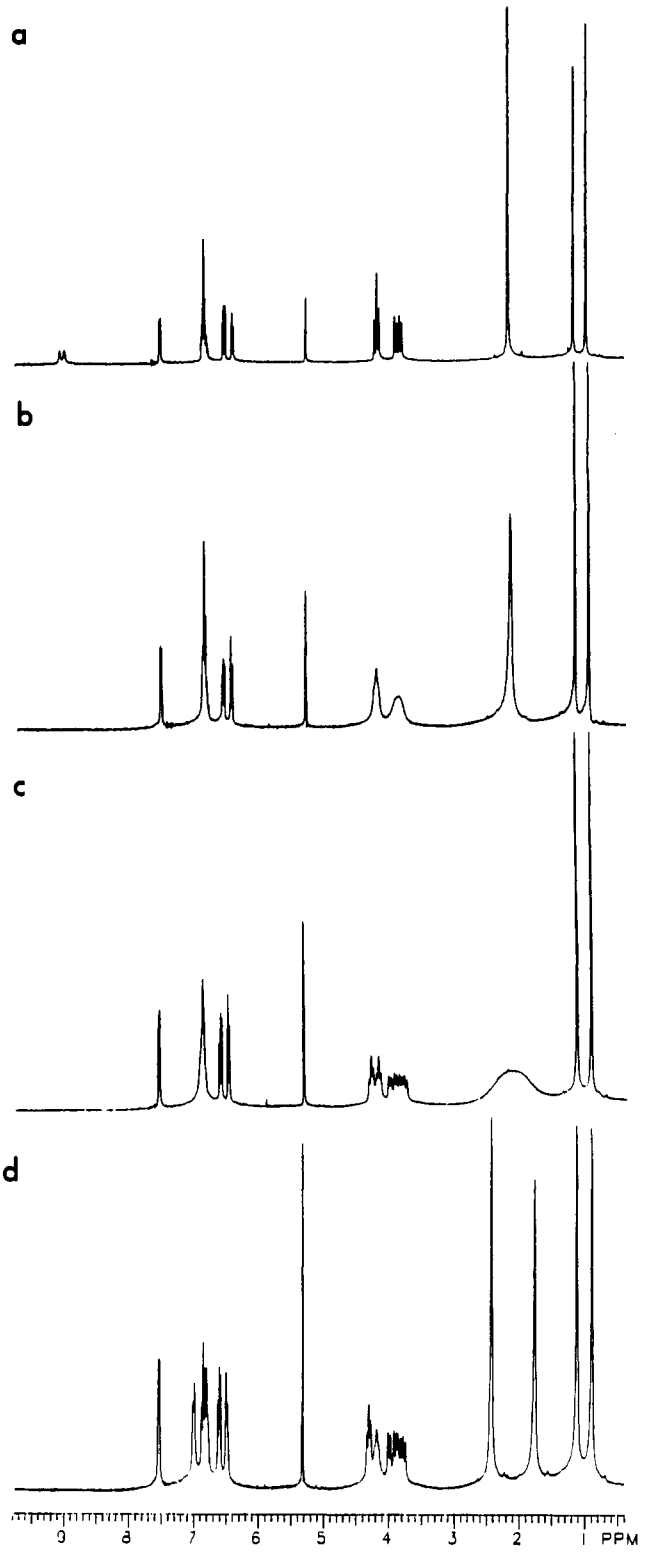

Figure 7. Variable-temperature ^1H NMR spectrum of **2** in CD_2Cl_2 at (a) 18.5 °C, (b) −8.0 °C, (c) −28.2 °C, and (d) −48.0 °C. The signal at 5.3 ppm is due to an impurity.

low-intensity doublet attributable to the hydrogen-bonded NH proton. The methylene multiplets are assigned to two types of protons corresponding to two ABX quartets where the lower field 1:2:1 triplet results from overlapping doublets. In the ^1H spectrum of the phosphate, **3**, at 17.5 °C, the latter pattern is resolved showing two quartets in this region indicating the presence of two methylene protons. In addition, the spectrum of **3** at 17.5 °C shows two types of phosphorinane ring methyls and one type of xylyloxy methyl group. The spectrum is consistent with retention of the solid-state structure in solution with rapid rotation of the

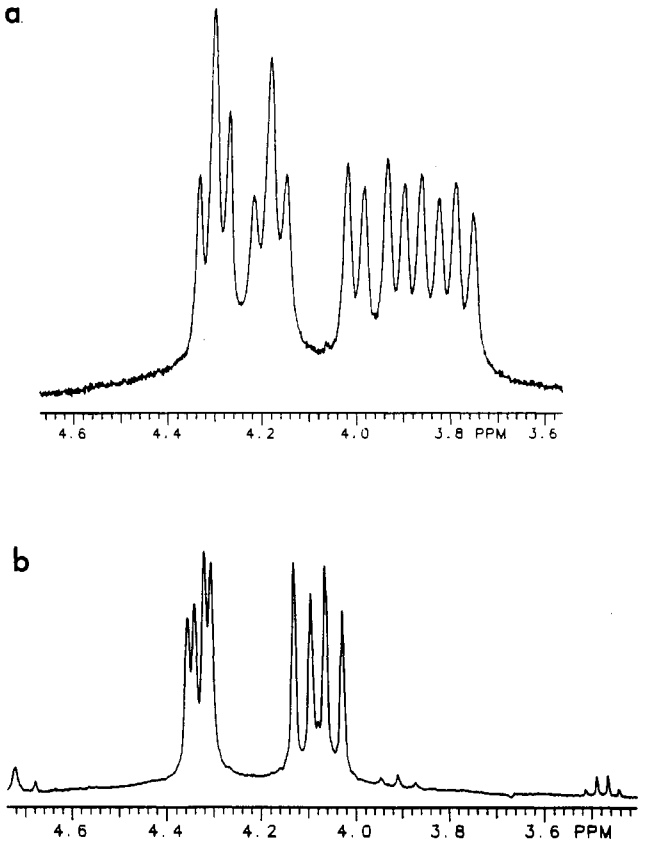

Figure 8. (a) Expansion of the ^1H NMR spectrum of **2** in CD_2Cl_2 at −38 °C, showing the phosphorinane ring methylene proton region. (b) Partial ^1H NMR spectrum of phosphate **3** in $CDCl_3$ at 17.5 °C, depicting the phosphorinane ring methylene region.

xylyl groups about the C–O bond.

The spectrum of **2** in Figure 7 and its variable-temperature behavior are similar to those discussed for A–C[12] as well as **1** and **4**. On cooling, ligand exchange is inhibited causing the appearance of two xylyloxy methyl signals (indicating the cessation of rotation of the xylyl group about the C–O bond) and two multiplets in the phosphorinane methylene region, which contains eight lines in the higher field multiplet and six lines in the lower field multiplet. An expansion of this region is displayed in Figure 8. These multiplets correspond to the presence of four distinct types of methylene protons (rather than two at the higher temperatures), giving a pattern of four ABX quartets where the intensity distribution of 1:2:1:1:2:1 in the lower field multiplet is assumed to arise from overlapping doublets. Intramolecular ligand exchange is implied by retention of $^3J_{P-H}$ coupling for the ring methylene proton signals over the temperature range studied for **1**, **2**, and **4**. During these spectral changes, the number of phosphorinane methyl signals remains invariant at two.

Activation energies, ΔG^* (Table VIII), corresponding to ligand exchange for trigonal bipyramids of **1**, **2**, and **4** fall in a narrow range, 10.5–12.6 kcal/mol, as might be expected for these closely related structures. The pathway indicated is one which places the six-membered ring diequatorially in an exchange intermediate following a Berry pseudorotational process[22] involving intervening square pyramids. This is the same process elaborated on for exchange in A–C.[12] It allows the four ring methylene protons and two xylyloxy protons present at lower temperatures to average to two ring methylene protons and one xylyloxy proton on warming while maintaining two kinds of phosphorinane ring methyl groups. For these phosphoranes, the range of activation energies was even more narrow, 10.3–11.5 kcal/mol, and is seen to overlap with the present values for **1**, **2**, and **4**.

Conclusion

The incorporation of hydrogen bonding via NH groups is found to make use of donor functions attached to five-membered rings

of tetraoxyphosphoranes rather than the use of P–O ring-bound oxygen atoms as studied previously.[12] In either case, chain and dimer formations resulted for the pentacoordinated spirocyclic phosphorus compounds with the rings situated axial–equatorially in trigonal-bipyramidal geometries. In contrast to the previous study[12] where hydrogen bonding gave boat and chair conformations for the six-membered ring, the present study gave chair conformations exclusively. Activation energies for intramolecular exchange interpreted in terms of a pseudorotational process requiring diequatorial placement of the phosphorinane ring in a TBP exchange intermediate were similar for the two classes of hydrogen-bonded compounds and suggested that the energy required for diequatorial placement of a phosphorinane ring (≥11 kcal/mol) in the ground state exceeds the available hydrogen-bond energy. Thus far, no evidence from solid-state studies has been obtained supporting a diequatorial orientation for a six-membered ring in an oxyphosphorane. These results suggest that if protein kinases in their interaction with *c*-AMP are capable of providing the energy necessary for the formation of phosphorane activated states proposed to contain (e-e) orientations,[13,15,16] a combination of active-site constraints may be required.

Acknowledgment. The support of this research by the National Science Foundation (Grant CHE88-19152) and the Army Research Office is gratefully acknowledged as is a helpful discussion with Professor W. E. McEwen.

Registry No. **1**, 135929-32-7; **2**, 135929-33-8; **3**, 24418-67-5; **4**, 135929-34-9; **5**, 74390-22-0; 2-amino-5-nitrophenol, 121-88-0; 2-amino-3-hydroxypyridine, 16867-03-1; 2-hydroxybenzyl alcohol, 90-01-7; 2-amino-4,6-dimethylphenol, 41458-65-5.

Supplementary Material Available: Tables of atomic coordinates, thermal parameters, additional bond lengths and angles, and hydrogen atom parameters (Tables S1–S4 for **1**, Tables S5–S8 for **2**, and Tables S9–S12 for **3**) (25 pages); listings of structure factors (25 pages). Ordering information is given on any current masthead page.

Contribution from the Department of Chemistry of the University of Florence, Florence, Italy, and Departement de Recherche Fondamentale, Centre d'Etudes Nucleaires de Grenoble, Grenoble, France

Structure and Magnetic Ordering of a Ferrimagnetic Helix Formed by Manganese(II) and a Nitronyl Nitroxide Radical

Andrea Caneschi,[†] Dante Gatteschi,*[,†] Paul Rey,[‡] and Roberta Sessoli[†]

Received February 13, 1991

A chain compound of formula $Mn(hfac)_2NITPhOMe$, where hfac = hexafluoroacetylacetonato and NITPhOMe = 2-(4-methoxyphenyl)-4,4,5,5-tetramethylimidazoline-1-oxyl 3-oxide, was synthesized, and the X-ray analysis showed that it crystallizes in the trigonal acentric $P3_1$ space group with a = 11.131 (3) Å, c = 20.846 (9) Å, and Z = 3. The structure consists of helices in which the $Mn(hfac)_2$ moieties are bridged by the radicals coordinated through the two equivalent oxygen atoms. The magnetic susceptibility in the form χT vs T shows a marked increase on lowering the temperature, and a numerical fitting indicated a strong antiferromagnetic intrachain interaction (J = 344 cm^{-1}). The uncompensation of the $S = {}^5/_2$ spin of manganese(II) and $S = {}^1/_2$ spin of the radical originates high resultant magnetic moments, and at ca. 4.8 K the system orders three-dimensionally as confirmed by AC susceptibility measurements in nearly zero field. Magnetization measurements indicate that the system orders ferrimagnetically with S = 2, as expected for antiparallel alignment of $S = {}^5/_2$ and $S = {}^1/_2$. Single-crystal EPR spectra at variable temperatures revealed a pure xy anisotropy with the easy plane perpendicular to the helix axis c. The calculation of the dipolar anisotropy performed within the point dipole approximation reproduces the observed behavior. The transition temperature and the dipolar energies are compared with those of two other $Mn(hfac)_2NITR$ chains, and magneto–structural correlations that justify the experimental trend in critical temperature are presented. The acentric space group allows nonlinear optical activity, and preliminary measurements show a sizeable SHG activity at 1064 nm, which must essentially be associated with the radical.

Introduction

Molecular based magnetic materials are compounds exhibiting spontaneous magnetization below a critical temperature, T_c, that are formed by molecular entities, even if they do not necessarily correspond to molecular lattices. Beyond the challenge of designing and synthesizing new classes of compounds it is hoped that the properties of these materials can be finely tuned by exploiting the techniques of molecular chemistry.[1-7] Since the magnetic properties are determined by the spatial arrangement of the interacting magnetic centers, it is necessary to learn the most appropriate ways of assembling them in a lattice in order to maximize the interactions.

A potentially interesting feature of these materials is that in principle they might show an unusual association of properties, for instance magnetic and optical, magnetic and electrical, and magnetic and chemical, that are bound to their molecular nature.[8] This is a field that has not yet been fully exploited and deserves much attention. In particular, since among the possible uses that can be envisaged for molecular based magnetic materials exhibiting spontaneous magnetization, magneto–optical effects are of paramount interest, it is very important to design materials that can show unusual optical properties associated with spontaneous magnetization.

We are currently studying materials that are formed by the interaction of metal ions and nitronyl nitroxides of formula 2-R-4,4,5,5-tetramethylimidazoline-1-oxyl 3-oxide, NITR.[7] In this

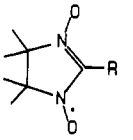

NITR

approach to molecular based magnetic materials the versatility is given by the possibility to change the metal ion and the R group

[†] University of Florence.
[‡] Centre d'Etudes Nucleaires de Grenoble.

(1) Miller, J. S.; Epstein, A. J.; Reiff, W. M. *Chem. Rev.* **1988**, *88*, 201. Miller, J. S.; Epstein, A. J.; Reiff, W. M. *Acc. Chem. Res.* **1988**, *21*, 114.
(2) Kahn, O. *NATO ASI Ser. B* **1987**, *168*, 93. Nakatani, K.; Carriat, J. Y.; Journaux, Y.; Kahn, O.; Lloret, F.; Renard, J. P.; Pei, Y.; Sletten, J.; Verdaguer, M. *J. Am. Chem. Soc.* **1989**, *111*, 5739.
(3) Korshak, Y. V.; Medvedeva, T. V.; Ovchinnikov, A. A.; Spector, V. N. *Nature* **1987**, *326*, 370.
(4) Iwamura, H. *Pure Appl. Chem.* **1986**, *58*, 187.
(5) Le Page, T. J.; Breslow, R. *J. Am. Chem. Soc.* **1987**, *109*, 6412.
(6) Torrance, J. B.; Oostra, S.; Nazzal, A. *Synth. Met.* **1987**, *19*, 708.
(7) Caneschi, A.; Gatteschi, D.; Sessoli, R.; Rey, P. *Acc. Chem. Res.* **1989**, *22*, 329.
(8) Miller, J. S. *Adv. Mater.* **1990**, *2*, 98.

0020-1669/91/1330-3936$02.50/0